

**Self-diffusion in a system of interacting Langevin particles**D. S. Dean<sup>1,2</sup> and A. Lefèvre<sup>3</sup><sup>1</sup>*DAMTP, CMS, University of Cambridge, Cambridge CB3 0WA, United Kingdom*<sup>2</sup>*IRSAMC, Laboratoire de Physique Théorique, Université Paul Sabatier, 118 route de Narbonne, 31062 Toulouse Cedex 04, France*<sup>3</sup>*Rudolf Peierls Centre for Theoretical Physics, 1 Keble Road, Oxford, OX1 3NP, United Kingdom*

(Received 15 January 2004; published 23 June 2004)

The behavior of the self-diffusion constant of Langevin particles interacting via a pairwise interaction is considered. The diffusion constant is calculated approximately within a perturbation theory in the potential strength about the bare diffusion constant. It is shown how this expansion leads to a systematic double expansion in the inverse temperature  $\beta$  and the particle density  $\rho$ . The one-loop diagrams in this expansion can be summed exactly and we show that this result is exact in the limit of small  $\beta$  and  $\rho\beta$  constants. The one-loop result can also be resummed using a semiphenomenological renormalization group method which has proved useful in the study of diffusion in random media. In certain cases the renormalization group calculation predicts the existence of a diverging relaxation time signaled by the vanishing of the diffusion constant, possible forms of divergence coming from this approximation are discussed. Finally, at a more quantitative level, the results are compared with numerical simulations, in two dimensions, of particles interacting via a soft potential recently used to model the interaction between coiled polymers.

DOI: 10.1103/PhysRevE.69.061111

PACS number(s): 05.40.-a, 05.60.-k, 66.10.-x

**I. INTRODUCTION**

Transport properties of deeply cooled liquids may change by several orders of magnitude when one reduces the temperature [1]. Indeed, a liquid undergoing a deep quench below its melting transition may stay in a metastable supercooled state. In this state, the relaxation time is much larger than the experimental time scale, and the system is always out of equilibrium. Experiments suggest that in “fragile” glass formers, there is a temperature  $T_0$  at which the relaxation time diverges. Even if the mere existence of a divergence of the relaxation time  $\tau$  at finite temperature is still controversial, the experimental data can be often fitted by the so-called Vogel-Fulcher-Tammann law  $\tau \sim \exp[A/(T-T_0)]$ . Since such a glassy behavior has been observed in a wide range of materials, there have been huge efforts dedicated to computing the transport properties in supercooled liquids. Among them, the mode coupling theory (MCT) [2–4] appears to give results and predictions which fit remarkably well with data for many different systems [5]. However, despite its successes, the derivation of MCT either from the Mori-Zwanzig formalism [4] or from fluctuating hydrodynamics [6] remains quite obscure, and systematic improvements seem difficult to implement and control. Hence, with the aim of understanding better the structure of the dynamics, alternative methods of computing transport properties of systems of many interacting particles such as supercooled liquids are worth examining. In this paper, we will develop a method to compute the long time self-diffusion constant which allows systematic double perturbative expansions, in the strength of the interaction and in the density of particles. The approach is based on the Langevin dynamics for  $N$  particles with two-body interactions, though this approach may be generalized easily to three-body interactions. Such Markovian Langevin dynamics can be invoked in liquids over length and time scales where inertial effects become negli-

gible. The Langevin equation thus represents a coarse grained image of the system and the effective parameters and interactions used in the Langevin approach require microscopic derivation. The Langevin approach also naturally describes the dynamics of colloids in solution [7], the Brownian noise is induced by the solvent and the effective interaction between particles is composed of a pairwise direct interaction between the colloids plus additional hydrodynamic interactions induced via the solvent.

We consider the interacting set of Langevin equations for particles  $\mathbf{X}_i$  interacting via a pairwise potential  $V(\mathbf{X}_i - \mathbf{X}_j)$  depending only on the distance between the particles at temperature  $T$  in  $D$  dimensions:

$$\frac{d\mathbf{X}_i^\alpha}{dt} = -\lambda \sum_j \partial_{X_i^\alpha} V(\mathbf{X}_i - \mathbf{X}_j) + \eta_i^\alpha. \quad (1)$$

The units of time are chosen such that the white noise field  $\eta_i^\alpha$  has the correlation function

$$\langle \eta_i^\alpha(t) \eta_j^\beta(t') \rangle = 2\kappa \delta_{ij} \delta^{\alpha\beta} \delta(t - t'), \quad (2)$$

where the angled brackets indicate averaging over the thermal noise. The term  $\kappa$  is thus the bare diffusion constant of the particles in the absence of interactions. The fluctuation dissipation theorem or Einstein relation implies that  $\lambda/\kappa = 1/T$ . This system of equations can be used to describe a colloidal system of interacting particles suspended in solution when hydrodynamic interactions are neglected. The neglecting of hydrodynamic interactions is justified where the direct two body interaction  $V$  is of much longer range than the hydrodynamic interactions. A commonly cited example is charged colloids in a solution when the Debye length is very large with respect to the particle sizes.

The effective macroscopic diffusion constant  $\kappa_e$  of particle  $i$  is defined by

$$\lim_{t \rightarrow \infty} \langle X_i^2(t) \rangle = 2D\kappa_e t. \quad (3)$$

It is the aim of this paper to develop a technique for the calculation of  $\kappa_e$ . There are two basic routes to calculate  $\kappa_e$ . The first is based on the direct calculation of the diffusion constant [8–19]. The second is based on the calculation of the modification of the response to a small external force on a given particle due to the interaction with the other particles, the so-called relaxation effect; the resulting value of  $\kappa_e$  is then determined from the Einstein or fluctuation dissipation relation [20–23]. One approach to studying the dynamics of a tracer particle is to write an effective one particle Langevin equation with a non-Markovian memory kernel, derived via projection operator techniques [8–13,16,17,23,19]. This kernel must then be computed by invoking approximation or closure schemes such as mode coupling-like approximations [15,16], cluster expansions [13], or weak coupling expansions [8,17,18]. Other approaches are based on closure schemes for the Smoluchowski equation [9–11,21,22], which normally involve closing the hierarchy of equations for the joint probability density functions by replacing, for instance, the three body joint probability density function by its corresponding Kirkwood superposition approximation. Both techniques can be handled to produce results which are exact to first order in the particle density  $\rho$  [12–14,20,23].

The paper is organized as follows. In Sec. II we develop the diagrammatic perturbation theory for the calculation of the self-diffusion constant. In Sec. III the one-loop analysis and its renormalization group resummation are developed and the physical consequences of their predictions are discussed. In Sec. IV a brief comparison of the results of various calculational schemes and numerical simulations is presented for the case of a soft potential. The bulk of the discussion of the physics is to be found in Secs. III and IV and in the Conclusion.

## II. DIAGRAMMATIC EXPANSION

Here we use a technique based on a perturbative weak coupling expansion of the Smoluchowski or Fokker-Planck equation for the  $N$  particles in interaction. The form of this perturbation expansion is identical to that used to calculate the effective diffusion constant of a particle in a random potential. We denote by  $P(\mathbf{x}_1, \mathbf{x}_2, \dots, \mathbf{x}_N, t)$  the probability density function for the particle displacements from their original positions at  $t=0$  at time  $t$ , that is to say the density of  $\{\mathbf{X}_i(t) - \mathbf{X}_i(0); 1 \leq i \leq N\}$ . We take initial conditions  $\mathbf{X}_i(0) = \mathbf{x}_i^{(0)}$  where the  $\mathbf{x}_i^{(0)}$  are independently and uniformly distributed throughout the volume  $V$  of the system. In principle one could take other initial conditions for the  $\mathbf{x}_i^{(0)}$ , notably one could take their equilibrium distribution. However, if the system is ergodic then the resulting behavior of the diffusion effective constant should be independent of this distribution. The disorder induced by the random initial conditions shows the link with diffusion in a random potential. The forward Fokker-Planck or generalized Smoluchowski equation for  $P$  is

$$\frac{\partial P}{\partial t} = \kappa \nabla^2 P + \lambda \nabla \cdot (P \nabla \phi), \quad (4)$$

where  $\nabla$  is the gradient operator on  $\mathbb{R}^{DN}$  where  $D$  is the spatial dimension and  $N$  the number of particles. The potential  $\phi$  in this formalism is given by

$$\phi(\mathbf{x}_1, \mathbf{x}_2, \dots, \mathbf{x}_N) = \phi_0(\mathbf{x}_1 + \mathbf{x}_1^{(0)}, \mathbf{x}_2 + \mathbf{x}_2^{(0)}, \dots, \mathbf{x}_N + \mathbf{x}_N^{(0)}), \quad (5)$$

where

$$\phi_0(\mathbf{x}_1, \mathbf{x}_2, \dots, \mathbf{x}_N) = \sum_{i < j} V(\mathbf{x}_i - \mathbf{x}_j). \quad (6)$$

From here on we shall denote by the vector  $\mathbf{x}$ , without a particle index, the global position vector  $(\mathbf{x}_1, \mathbf{x}_2, \dots, \mathbf{x}_N)$  in  $\mathbb{R}^{DN}$  and by the vector  $\mathbf{k}$  the corresponding Fourier vector  $(\mathbf{k}_1, \mathbf{k}_2, \dots, \mathbf{k}_N)$ . If one defines

$$\tilde{P}(\mathbf{k}, s) = \int_0^\infty dt \int_{\mathbb{R}^{DN}} d\mathbf{x} \exp(-st - i\mathbf{k} \cdot \mathbf{x}) P(\mathbf{x}, t), \quad (7)$$

it is straightforward to show that  $\tilde{P}(\mathbf{k}, s)$  obeys

$$\tilde{P}(\mathbf{k}, s) = \frac{1}{\kappa \mathbf{k}^2 + s} - \frac{\lambda}{\kappa \mathbf{k}^2 + s} \int_{\mathbb{R}^{DN}} \frac{d\mathbf{q}}{(2\pi)^{ND}} \mathbf{k} \cdot \mathbf{q} \tilde{\phi}(\mathbf{q}) \tilde{P}(\mathbf{k} - \mathbf{q}, s). \quad (8)$$

We note that because of our choice of coordinates relative to the initial conditions,  $P(\mathbf{x}, 0) = \delta(\mathbf{x})$  and also

$$\tilde{\phi}(\mathbf{q}) = \exp(i\mathbf{q} \cdot \mathbf{x}^{(0)}) \tilde{\phi}_0(\mathbf{q}). \quad (9)$$

One has also that

$$\tilde{\phi}_0(\mathbf{q}) = (2\pi)^{(N-1)D} \tilde{\psi}_0(\mathbf{q}), \quad (10)$$

with

$$\tilde{\psi}_0(\mathbf{q}) = \sum_{i < j} \tilde{V}(\mathbf{q}_i) \delta(\mathbf{q}_i + \mathbf{q}_j) \prod_{k \in \{i, j\}} \delta(\mathbf{q}_k). \quad (11)$$

Using these definitions one obtains the equation

$$\begin{aligned} \tilde{P}(\mathbf{k}, s) &= \frac{1}{\kappa \mathbf{k}^2 + s} - \frac{\lambda}{\kappa \mathbf{k}^2 + s} \int_{\mathbb{R}^{DN}} \frac{d\mathbf{q}}{(2\pi)^D} \mathbf{k} \cdot \mathbf{q} \tilde{\psi}_0(\mathbf{q}) \\ &\times \exp(i\mathbf{q} \cdot \mathbf{x}^{(0)}) \tilde{P}(\mathbf{k} - \mathbf{q}, s). \end{aligned} \quad (12)$$

Equation (12) can be solved iteratively leading to the expansion which is represented in Fig. 1. We note here that this weak coupling expansion as it stands only makes sense for potentials which are bounded as  $V(\mathbf{x})$  is treated as a small perturbation. However the series can be resummed to obtain physical results for unbounded (such as hard core) potentials. In addition the behavior of soft potentials is of direct physical interest as they provide coarse grained descriptions of coiled polymers [25], star polymers [26], and micelles [27] in solvents.

Momentum is conserved at each vertex and the Feynman rules are the following:

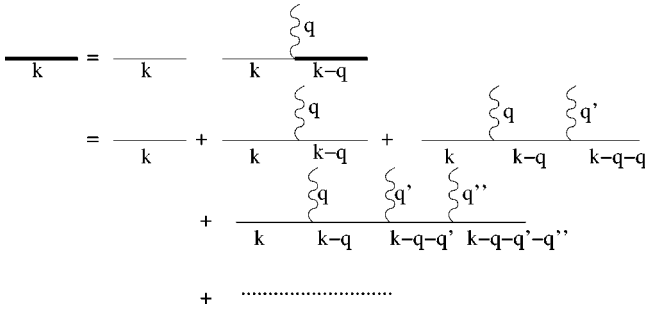


FIG. 1. Diagrammatic expansion for  $\tilde{P}(\mathbf{k},s)$ .

Each solid line (horizontal) corresponds to the bare Green's function corresponding to the system of particles in the absence of interactions

$$G_0(\mathbf{k},s) = \frac{1}{\kappa\mathbf{k}^2 + s}, \quad (13)$$

where  $\mathbf{k}$  is the momentum in that line.

Each vertex (vertical wavy line) carries a factor

$$-\lambda \mathbf{k} \cdot \mathbf{q} \psi_0(\mathbf{q}) \exp(i\mathbf{q} \cdot \mathbf{x}^{(0)}), \quad (14)$$

where  $\mathbf{k}$  is the ingoing momentum (from the left) and  $\mathbf{q}$  is the momentum flowing into the vertical wavy line.

Each momentum  $\mathbf{q}$  flowing into a wavy line is integrated over  $R^{DN}$  with the measure  $d\mathbf{q}/(2\pi)^D$ .

We see that the ingoing and outgoing momentum on each of the generated diagrams is not conserved. This is because the spatial translational invariance of the system is not explicit. To study a spatially translational invariant system we average over the initial position  $\mathbf{x}^{(0)}$  throughout the volume  $V^N$ . We shall take uniform initial conditions although any initial conditions which have the property of spatial translational invariance should give the same asymptotic (late time) properties for  $G(\mathbf{k},s) = \langle \tilde{P}(\mathbf{k},s) \rangle_0$ . Here the angled brackets with the 0 subscript indicate the average over the initial position vector  $\mathbf{x}^{(0)}$  and is defined by

$$\langle A \rangle_0 = \frac{1}{V^N} \int_{V^N} d\mathbf{x}^{(0)} A(\mathbf{x}^{(0)}). \quad (15)$$

In the limit of large  $V$  this integration multiplies each diagram by a factor of  $(2\pi)^{ND} \delta(\sum_v \mathbf{q}_v) / V^N$  where the  $\mathbf{q}_v$  are all the momenta flowing into the upward wavy lines in each diagram at each vertex  $v$ . This momentum conservation ensures that the momentum flowing into each diagram is the same as that flowing out and indicates the invariance by translation in space of the system averaged over its initial conditions. After taking this average over the diagrams in Fig. 1 we obtain the diagrammatic expansion for  $G(\mathbf{k},s)$ . The Feynman rules are as before but with the following modifications:

Each diagram carries an overall factor of  $(2\pi)^{(N-1)D} / V^N$ .

There are only  $n-1$  independent momenta for each diagram of  $n$  vertices by momentum conservation. Each of these momenta is integrated with the measure  $d\mathbf{q}/(2\pi)^D$  as before.

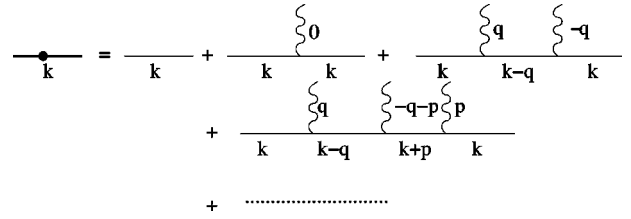


FIG. 2. Diagrammatic expansion of  $G(\mathbf{k},s)$  (shown as a line with a closed circle) obtained after averaging over initial particle positions in the diagrammatic expansion shown in Fig. 1.

The form of the perturbation expansion shown in Fig. 2 shows that one can write  $G(\mathbf{k},s)$  as

$$G(\mathbf{k},s) = \frac{1}{\kappa\mathbf{k}^2 + s} + \frac{1}{(\kappa\mathbf{k}^2 + s)^2} D(\mathbf{k},s). \quad (16)$$

The term  $D(\mathbf{k},s)$  can clearly be expressed in terms of one-particle-irreducible diagrams. Diagrams which are one-particle-reducible are those containing a bare Green's function having a pure momentum  $\mathbf{k}$  flowing through one of their bare Green's functions and can thus be factorized. The bare Green's function connecting two one-particle-irreducible diagrams is therefore  $1/(\kappa\mathbf{k}^2 + s)$ . If we denote the one-particle-irreducible diagram contribution as  $\Sigma(\mathbf{k},s)$  then

$$G(\mathbf{k},s) = \frac{1}{\kappa\mathbf{k}^2 + s} + \frac{\Sigma(\mathbf{k},s)}{(\kappa\mathbf{k}^2 + s)^2} + \frac{\Sigma(\mathbf{k},s)^2}{(\kappa\mathbf{k}^2 + s)^3} + \dots, \quad (17)$$

which sums to give

$$G(\mathbf{k},s) = \frac{1}{\kappa\mathbf{k}^2 - \Sigma(\mathbf{k},s) + s}. \quad (18)$$

We now note that by the conservation of probability  $G(0,s) = 1/s$  and we thus expect that for small  $|\mathbf{k}|$ ,

$$G(\mathbf{k},s) = \frac{1}{\kappa\mathbf{k}^2 - \mathbf{k}^2 E(s) + s}, \quad (19)$$

where  $\Sigma(\mathbf{k},s) \approx \mathbf{k}^2 E(s)$ . In the limit of small  $|\mathbf{k}|$  and  $s$  therefore

$$G(\mathbf{k},s) = \frac{1}{[\kappa - E(0)]\mathbf{k}^2 + s}. \quad (20)$$

The effective diffusion constant for the particles is extracted using the fact that

$$2D\kappa_e t = \lim_{t \rightarrow \infty} \langle [\mathbf{X}_i(t) - \mathbf{x}_i^{(0)}]^2 \rangle, \quad (21)$$

where the angled brackets on the right-hand side above indicate the average over the thermal noise and over the initial conditions. We also have that

$$G(\mathbf{k},s) = \int_0^\infty dt \exp(-st) \left\langle \exp\left(-i \sum_i \mathbf{k}_i \cdot [\mathbf{X}_i(t) - \mathbf{x}_i^{(0)}]\right) \right\rangle. \quad (22)$$

For small  $s$  in Laplace space we have

$$\int_0^\infty dt \exp(-st) \langle [\mathbf{X}_i(t) - \mathbf{x}_i^{(0)}]^2 \rangle \approx \int_0^\infty dt \exp(-st) 2D\kappa_e t$$

$$= \frac{2D\kappa_e}{s^2} \quad (23)$$

and therefore, from Eq. (22), for small  $s$ ,

$$\frac{2D\kappa_e}{s^2} \approx - \sum_{\alpha=1}^D \left. \frac{\partial^2}{\partial k_i^{\alpha 2}} G(\mathbf{k}, s) \right|_{\mathbf{k}=0}. \quad (24)$$

Now using Eq. (20) we obtain

$$\kappa_e = \kappa - E(0). \quad (25)$$

The calculation of  $\kappa_e$  can therefore be evaluated from  $G(\mathbf{k}, 0)$ . We may express the term  $E(0)$  as an expansion in the number of vertices  $\nu$  in the diagram, we write

$$E(0) = \sum_\nu E_\nu, \quad (26)$$

where

$$E_\nu = \lim_{|\mathbf{k}| \rightarrow 0} \frac{1}{\mathbf{k}^2} \sum_\nu (\mathbf{k}, 0), \quad (27)$$

where  $\sum_\nu(\mathbf{k})$  is the sum of one-particle-irreducible diagrams with  $\nu$  vertices. From Fig. 2 we may write

$$G(\mathbf{k}, 0) = \frac{1}{\kappa \mathbf{k}^2} + \frac{1}{(\kappa \mathbf{k}^2)^2} \sum_\nu D_\nu(\mathbf{k}, 0), \quad (28)$$

where  $D_\nu(\mathbf{k}, 0)$  is the sum over all terms with  $\nu$  vertices and not just the one-particle-irreducible ones. The one-particle-irreducible components of  $D_\nu(\mathbf{k}, 0)$ ,  $\sum_\nu(\mathbf{k}, 0)$ , must be extracted from  $D_\nu(\mathbf{k}, 0)$ . The terms  $D_\nu(\mathbf{k}, 0)$  have the behavior  $D_\nu(\mathbf{k}, 0) \approx F_\nu \mathbf{k}^2$  for small  $|\mathbf{k}|$ . It is straightforward to verify that the term  $F_1$  is zero. This means therefore that there is no contribution to  $O(\lambda)$  in the asymptotic single particle diffusion constant  $\kappa_e$ . Examining Fig. 2 we find that

$$D_2(\mathbf{k}, 0) = \frac{(2\pi)^{D(N-2)}}{\kappa V^N} \lambda^2 \int_{\mathbb{R}^{DN}} d\mathbf{q} \frac{\mathbf{k} \cdot \mathbf{q}(\mathbf{k} - \mathbf{q})}{(\mathbf{k} - \mathbf{q})^2} \psi_0(\mathbf{q}) \psi_0(-\mathbf{q}). \quad (29)$$

The potential term in the integrand may be expressed using Eq. (11) as

$$\psi_0(\mathbf{q}) \psi_0(-\mathbf{q}) = \sum_{i < j} \sum_{k < l} \tilde{V}(\mathbf{q}_i) \tilde{V}(-\mathbf{q}_k) \delta(\mathbf{q}_i + \mathbf{q}_j) \delta(\mathbf{q}_k + \mathbf{q}_l)$$

$$\times \prod_{r \in \{i, j\}} \delta(\mathbf{q}_r) \prod_{s \in \{k, l\}} \delta(\mathbf{q}_s). \quad (30)$$

One must keep in mind that only terms with nonzero  $\mathbf{q}$  can contribute (one can imagine an additional term  $+s$  in the denominator for small  $s$  which is taken to zero at the end of the calculation). The only terms in Eq. (30) which have nonzero momentum are those where the pair  $(i, j) = (k, l)$ . In addition, the computation is simplified if one assumes  $\mathbf{k}_r = 0$  for  $r > 1$ . Clearly the coefficient of  $\mathbf{k}_1^2$  in  $\kappa \mathbf{k}^2 - \sum(\mathbf{k}, 0)$  is the

self-diffusion constant of particle 1 which is also the self-diffusion constant of any given particle. Hence for the purposes of the calculation of  $\kappa_e$  we can restrict ourselves to the case  $\mathbf{k} = (\mathbf{k}_1, 0, 0, \dots, 0)$ . In this case, the only choices of the particle indices giving a nonzero diagram are  $i = k = 1$  and  $j = l$  due to the scalar product  $\mathbf{k} \cdot \mathbf{q}$  on the first vertex. There are thus  $N-1$  identical nonzero diagrams with two vertices. For notational simplicity in the following we will write  $\mathbf{k} = \mathbf{k}_1 \in \mathbb{R}^D$ . All the choices are equivalent to choosing  $\mathbf{q}_1 = \mathbf{q}$ ,  $\mathbf{q}_2 = -\mathbf{q}$  and  $\mathbf{q}_r = 0$  for  $r > 2$  where again  $\mathbf{q} \in \mathbb{R}^D$ . In the resulting integral there are repeated delta functions for the terms  $r = s$  and also a double  $\delta(\mathbf{q}_i + \mathbf{q}_j)$ . We use the relation for  $\mathbf{q} \in \mathbb{R}^D$ ,

$$\delta^2(\mathbf{q}) = \delta(\mathbf{q}) \frac{V}{(2\pi)^D}. \quad (31)$$

The result for  $D_2(\mathbf{k})$  is thus

$$D_2(\mathbf{k}, 0) = \frac{\lambda^2 \rho}{\kappa} \int_{\mathbb{R}^D} \frac{d\mathbf{q}}{(2\pi)^D} \frac{\mathbf{k} \cdot \mathbf{q} (2\mathbf{q} - \mathbf{k}) \cdot \mathbf{q}}{(\mathbf{k} - \mathbf{q})^2 + \mathbf{q}^2} \tilde{V}(\mathbf{q})^2. \quad (32)$$

The above diagram is also clearly one-particle-irreducible and hence  $F_2 = E_2$  thus giving

$$E_2 = \frac{1}{2} \frac{\lambda^2 \rho}{\kappa D} \int_{\mathbb{R}^D} \frac{d\mathbf{q}}{(2\pi)^D} \tilde{V}(\mathbf{q})^2 = \frac{1}{2} \frac{\lambda^2 \rho}{\kappa D} \int_{\mathbb{R}^D} d\mathbf{x} V^2(\mathbf{x}). \quad (33)$$

The diagram giving  $D_3(\mathbf{k}, 0)$  has the value

$$D_3(\mathbf{k}, 0) = - \frac{(2\pi)^{D(N-3)}}{\kappa^2 V^N} \lambda^3 \int_{\mathbb{R}^{DN}} d\mathbf{q} d\mathbf{p}$$

$$\times \frac{\mathbf{k} \cdot \mathbf{q}(\mathbf{k} - \mathbf{q}) \cdot (\mathbf{q} + \mathbf{p})(\mathbf{k} + \mathbf{p}) \cdot \mathbf{p}}{(\mathbf{k} - \mathbf{q})^2 (\mathbf{k} + \mathbf{p})^2}$$

$$\times \psi_0(\mathbf{q}) \psi_0(\mathbf{p}) \psi_0(-\mathbf{q} - \mathbf{p}). \quad (34)$$

To simplify the counting of diagrams with nonzero momentum let us consider the general expansion of  $\psi_0(\mathbf{q}_1) \cdots \psi_0(\mathbf{q}_n)$  in a diagram with  $n$  vertices. From Eq. (11) a given term on expanding the  $n$ -fold sum over pairs has the form

$$A_{i_1 j_1}(\mathbf{q}_1) \cdots A_{i_n j_n}(\mathbf{q}_n). \quad (35)$$

Any diagram where the momentum  $\mathbf{q}_v$  flowing into the vertex  $v$  is zero is due to the presence of the scalar product with  $\mathbf{q}_v$  at each vertex in the Feynman rules. The momentum flowing into the vertex  $v$  in the above decomposition over pairs is  $(0, 0, \dots, \mathbf{q}_i \cdots -\mathbf{q}_j \cdots 0, 0)$  i.e., it has  $\mathbf{q}_i$  at the particle position  $i$  and  $-\mathbf{q}_j$  at the particle position  $j$  in the total momentum vector. This is shown diagrammatically in Fig. 3.

Each horizontal line corresponds to a vertex and the horizontal coordinates are given by the points  $(i_v, j_v)$ . Each line must have a nonzero momentum, thus  $\mathbf{q}_v \neq 0$ . However, the sum of the momenta down each column must also be zero. Hence each coordinate  $i_v$  must appear on at least two lines in order to give a diagram which is nonzero. In Fig. 4 one example of the equivalent nonzero diagram contribution to  $E_2$  is shown. The three types of diagrams which give nonzero contributions to  $F_3$  are shown in Fig. 5. The diagrams of type 1 have a multiplicity of  $N-1$  and have the same particle pair

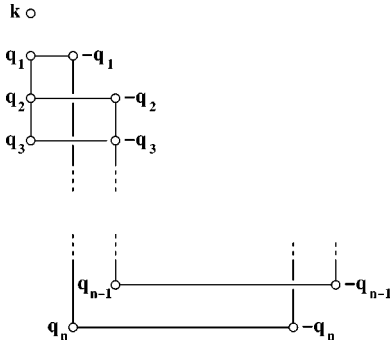


FIG. 3. Diagrammatic representation of the vertex momentum present in one term of the pair development of a product of  $\psi_0$ 's.

on each line. For the diagrams of type 2 and 3 there are  $(N-1)(N-2)$  diagrams of the precise form shown in the diagram. This is because there are  $N-1$  choices for the first pair (1,2) and  $N-2$  choices of the pair (2,3) (that is to say the particle number 3) shown on the second line. The choice of the last (third) pair is not free by momentum conservation. Due to the presence of a delta function  $\delta(\sum_v \mathbf{q}_i^v)$  for each column which is automatically satisfied when all the  $\mathbf{q}_i^v$  are zero, each empty column carries a factor of  $V/(2\pi)^D$ . Hence a diagram with  $k$  empty columns has a factor  $[V/(2\pi)^D]^k$ . In diagrams of type 1,  $k=N-2$  and in diagrams of type 2 and 3,  $k=N-3$ .

The contribution of diagrams of type 1 to  $D_3(\mathbf{k}, 0)$  is thus

$$D_3^{(1)}(\mathbf{k}, 0) = -\frac{\lambda^3 \rho}{\kappa^2} \int_{\mathbb{R}^{2D}} \frac{d\mathbf{q}}{(2\pi)^D} \frac{d\mathbf{p}}{(2\pi)^D} \times \frac{\mathbf{k} \cdot \mathbf{q} [(2\mathbf{q} - \mathbf{k}) \cdot (\mathbf{p} + \mathbf{q})] [(\mathbf{k} + 2\mathbf{p}) \cdot \mathbf{p}]}{[(\mathbf{k} - \mathbf{q})^2 + \mathbf{q}^2] [(\mathbf{k} + \mathbf{p})^2 + \mathbf{p}^2]} \times \tilde{V}(\mathbf{q}) \tilde{V}(\mathbf{p}) \tilde{V}(\mathbf{p} + \mathbf{q}), \quad (36)$$

which gives

$$F_3^{(1)} = -\frac{\lambda^3 \rho}{2D\kappa^2} \int_{\mathbb{R}^{2D}} \frac{d\mathbf{q}}{(2\pi)^D} \frac{d\mathbf{p}}{(2\pi)^D} \tilde{V}(\mathbf{q}) \tilde{V}(\mathbf{p}) \tilde{V}(\mathbf{p} + \mathbf{q}) \times \left( 1 - \frac{(\mathbf{p} \cdot \mathbf{q})^2}{\mathbf{p}^2 \mathbf{q}^2} \right). \quad (37)$$

The contribution from diagrams of type 2 and 3 is

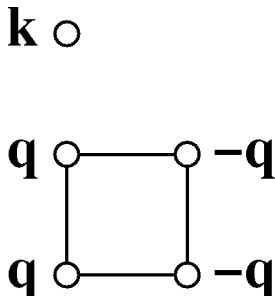


FIG. 4. Diagram in the pair development contributing to  $E_2$ .

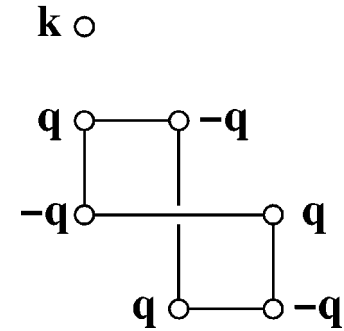
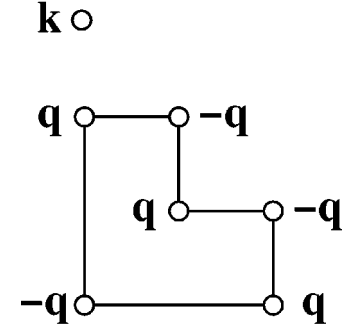
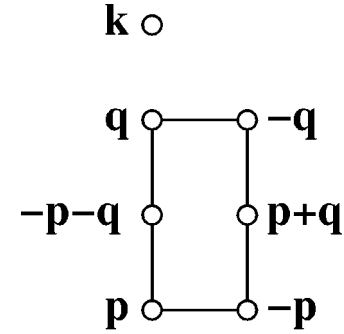


FIG. 5. Diagrams in the pair development contributing to  $E_3$  (top, type one; middle, type 2; and bottom, type 3).

$$F_3^{(2)} = -\frac{3\lambda^3 \rho^2}{4D\kappa^2} \int_{\mathbb{R}^D} \frac{d\mathbf{q}}{(2\pi)^D} \tilde{V}(\mathbf{q})^3. \quad (38)$$

These diagrams contributing to  $F_3$  are also one-particle-irreducible and hence to  $O(\lambda^3)$  we obtain

$$\frac{\kappa_e}{\kappa} = 1 - \frac{\rho\lambda^2}{2D\kappa^2} \int_{\mathbb{R}^D} \frac{d\mathbf{q}}{(2\pi)^D} \tilde{V}(\mathbf{q})^2 + \frac{\rho\lambda^3}{2D\kappa^3} \int_{\mathbb{R}^{2D}} \frac{d\mathbf{q}}{(2\pi)^D} \frac{d\mathbf{p}}{(2\pi)^D} \tilde{V}(\mathbf{q}) \tilde{V}(\mathbf{p}) \tilde{V}(\mathbf{q} + \mathbf{p}) \times \left( 1 - \frac{(\mathbf{p} \cdot \mathbf{q})^2}{\mathbf{p}^2 \mathbf{q}^2} \right) + \frac{3\rho^2 \lambda^3}{4D\kappa^3} \int_{\mathbb{R}^D} \frac{d\mathbf{q}}{(2\pi)^D} \tilde{V}(\mathbf{q})^3. \quad (39)$$

Hence the ratio  $\kappa_e/\kappa$  is expressed as a perturbation expansion in  $1/T$ . Notice here that there are more lines than rows in the diagrams of the pair development, which means that a finite number of diagrams contribute to any given order of the  $1/T$  expansion, whereas an infinite number of diagrams must be summed in order to compute any order in the  $\rho$

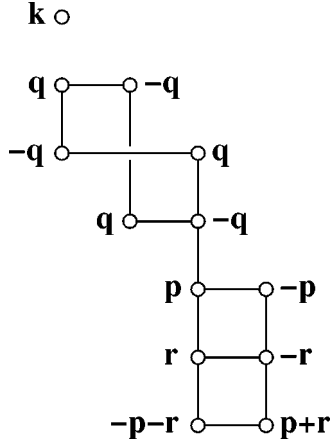


FIG. 6. Example of a diagram with disconnected loops in the pair development. Here the  $q$  loop is disconnected from the  $(p, r)$  loop.

expansion. A diagram with  $n$  lines and  $m$  nonempty columns is of order  $\rho^{m-1}(\lambda/\kappa)^n = \rho^{m-1}\beta^n$ , thus a systematic double expansion in  $\rho$  and  $\beta$  may be performed. We note that in Eq. (39) the leading order term in  $\beta$  which is of order  $\rho\beta^2$  recovers the weak coupling approximation. It is clear that the weak coupling approximation is not valid at low densities if the temperature is too low. The calculation of  $\kappa_e$  to first order in  $\rho$  involves summing all the diagrams which have just two columns occupied. These diagrams, which are all one-particle-irreducible, can be resummed via an integral equation [24] and one can show that the resulting expression for  $\kappa_e$  is the same as that given by the relaxation method applied to the effective two-body problem as expounded in [23].

Consider a diagram with  $v$  vertices and its  $\psi_0$  pair expansion. If the first  $v'$  vertices do not contain more than one-particle-index in common with the  $v-v'$  remaining vertices then the momentum flowing between the vertex  $v$  and  $v+1$  is zero (or  $\mathbf{k}$  if the column in common is the first one) and thus the diagram is zero (or one particle reducible). In other words, all diagrams with disconnected loops such as the one shown in Fig. 6 have a zero value or are one-particle-reducible and thus give no contribution to  $\kappa_e$ .

As an example, we consider potentials of the form

$$V(\mathbf{r}) = \frac{\epsilon}{(2\pi)^{D/2}} \exp\left(-\frac{r^2}{2r_0^2}\right), \quad (40)$$

which has been recently proposed to model the effective interaction between coiled polymers [25] at weak dilution. The Fourier transform of  $V(\mathbf{r})$  is then given by

$$\tilde{V}(\mathbf{q}) = \epsilon r_0^D \exp\left(-\frac{\mathbf{q}^2 r_0^2}{2}\right). \quad (41)$$

With this interaction potential and setting  $\epsilon=r_0=1$  we find from Eq. (39)

$$F_q^{(p)} = a_{pq} \rho^p T^{-q}, \quad (42)$$

where the first nonzero  $a_{pq}$ 's are

$$a_{12} = -\frac{1}{2^{D+1} D \pi^{D/2}},$$

$$a_{13} = \frac{1}{2D} \left( \frac{1}{3^{D/2}} - \frac{K(D) + DK(D+2)}{(2\pi)^D} \right),$$

$$a_{23} = \frac{3}{4D(6\pi)^{D/2}},$$

$$K(D) = \int_0^{1/\sqrt{3}} dx \frac{x^{D-1}}{1+x^2}. \quad (43)$$

Clearly this  $1/T$  expansion is valid only at very high temperature. It can be improved in several manners. One could compute higher orders in this expansion, which should give better agreement with the simulations, but, however, the expansion will inevitably break down at low  $T$ . Alternatively, one could try to sum infinite subseries in order to build approximate nonperturbative schemes. As mentioned above one approach is to try and resum the diagrams to obtain results exact for all  $\beta$  to order  $\rho$ . Here we shall concentrate on another resummation involving only one-loop diagrams.

### III. ONE-LOOP ANALYSIS

#### A. Simple one-loop contribution

Here we will focus on the class of one-loop diagrams. These diagrams are those which involve only one momentum integral. In this case, there are two dots on each occupied line or row and these diagrams are all one-particle-irreducible. In addition from the discussion in the previous section, these diagrams are the dominant ones in the limit where  $\rho\beta=c$  (with  $c$  a constant) and  $\rho \rightarrow \infty$ , or equivalently where  $\rho\beta=c$  and  $\beta \rightarrow 0$ . The dimensionless form of  $c$  would in fact be  $c' = \rho r_0^D \beta \epsilon$ , where  $r_0$  is the characteristic length scale of the potential and  $\epsilon$  its energy. As before, we write  $\mathbf{k}=\mathbf{k}_1 \in \mathbb{R}^D$ . The interesting point about this limit is that the (high temperature) statics of the model can also be evaluated [28], only chain diagrams in the virial expansion are retained in this limit. In electrolytic systems the Debye-Hückel approximation is recovered on the retention of only chain diagrams [29] and hence it is interesting that one can have a theory of  $\kappa_e$  for electrolyte systems which is compatible with the Debye-Hückel approximation which has proved so useful in the study of their static properties.

The typical one-loop diagrams can be reduced to the staircaselike diagrams shown in Fig. 7 by relabeling the particles. We note here that as we are summing an infinite number of diagrams one must be careful not to include the same particle twice in the same diagram as this will make the diagram two-loop. Hence for a finite system one cannot have a one-loop diagram with more than  $N$  vertices as it will include at least one particle [other than the tracer particle (1)] at least three times, meaning that the diagram can have at least two independent momenta flowing through it. In this case the counting of the one-loop diagrams with  $n$  vertices where  $n$  is of order  $N$  will be different. We have, however, taken the

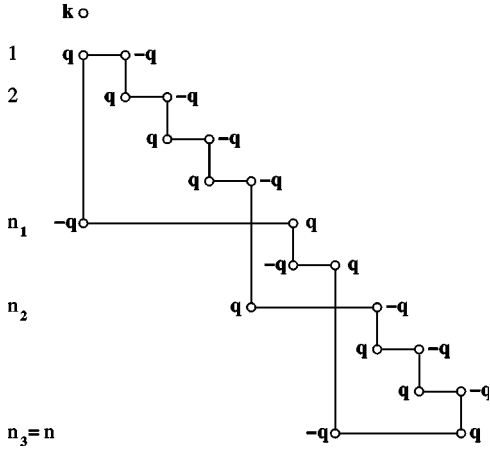


FIG. 7. Example of a staircase diagram contributing to the one-loop expansion.

limit  $N \rightarrow \infty$  already and hence this does not cause us any problems in the region where the power series giving the one-loop result is convergent.

In constructing a one-loop diagram at any level one must insert two points, one of which must coincide with one of the two unpaired (in the vertical direction) points above. The leftmost point of the new pair can either be paired with the rightmost of the two unpaired points above or it can be paired with the leftmost of the two unpaired points above, this gives a crossing. Clearly the first crossing must be back to the first column. Each diagram thus has  $p$  crossings where  $p \in [1, n-1]$ . If there is only one crossing then it must occur at level  $n$  corresponding to a staircase diagram with one crossing at the last line. Up to particle relabeling there is only one such diagram and its contribution is

$$b_1(n) = \frac{2n-3}{2^{n-1}D} \frac{\rho^{n-1}(-\lambda)^n}{\kappa^{n-1}} \int_{\mathbb{R}^D} \frac{d\mathbf{q}}{(2\pi)^D} \tilde{V}(\mathbf{q})^n. \quad (44)$$

If  $n > 2$  and  $p > 1$  then the first crossing must occur at the level  $n_1 \in [2, n-1]$ . At the level  $n_1+1$  the next two points can either cross or not cross just until the level  $n$  where the diagram most close. There are thus  $2^{n-1-n_1}$  topologically distinct diagrams with the same first crossing point at  $n_1$ . It is easy to see that these diagrams depend only on the position  $n_1$  of the first crossing (i.e., the second occurrence of the particle 1) and are given by

$$b_2(n_1, n) = \frac{n_1-2}{2^{n-2}D} \frac{\rho^{n-1}(-\lambda)^n}{\kappa^{n-1}} \int_{\mathbb{R}^D} \frac{d\mathbf{q}}{(2\pi)^D} \tilde{V}(\mathbf{q})^n. \quad (45)$$

Hence, taking into account all the multiplicities, the contribution of all the diagrams with  $n > 2$  lines is

$$\begin{aligned} b(n) &= b_1(n) + \sum_{n_1=2}^{n-1} 2^{n-n_1-1} b_2(n_1, n) \\ &= \frac{1-2^{1-n}}{D} \frac{\rho^{n-1}(-\lambda)^n}{\kappa^{n-1}} \int_{\mathbb{R}^D} \frac{d\mathbf{q}}{(2\pi)^D} \tilde{V}(\mathbf{q})^n. \end{aligned} \quad (46)$$

At  $n=2$  the above agrees with the result of Eq. (33), and

hence the above formula is valid for all  $n \geq 2$ . Performing the sum we find the one-loop contributions to be

$$\begin{aligned} \kappa_e^{(\text{one-loop})} - \kappa &= - \sum_n b(n) \\ &= - \frac{\rho\lambda^2}{D\kappa} \int_{\mathbb{R}^D} \frac{d\mathbf{q}}{(2\pi)^D} \tilde{V}(\mathbf{q})^2 \\ &\quad \times \left( \frac{1}{1 + \frac{\rho\lambda}{\kappa} \tilde{V}(\mathbf{q})} - \frac{1}{2} \frac{1}{1 + \frac{\rho\lambda}{2\kappa} \tilde{V}(\mathbf{q})} \right). \end{aligned} \quad (47)$$

The above may be conveniently rewritten in terms of  $c = \rho\lambda/\kappa$ ,

$$\kappa_e^{(\text{one-loop})} = \kappa \left[ 1 + \frac{1}{\rho D} \left( g(c) - 2g\left(\frac{c}{2}\right) \right) \right] \quad (48)$$

$$= \kappa \left[ 1 + \frac{\beta}{cD} \left( g(c) - 2g\left(\frac{c}{2}\right) \right) \right], \quad (49)$$

where

$$g(c) = \int_{\mathbb{R}^D} \frac{d\mathbf{q}}{(2\pi)^D} \frac{c \tilde{V}(\mathbf{q})}{1 + c \tilde{V}(\mathbf{q})}. \quad (50)$$

From the previous discussions the corrections to Eq. (49) are of the form

$$\kappa_e = \kappa_e^{(\text{one-loop})} + \beta^2 s_2(c) + \beta^3 s_3(c) \cdots \quad (51)$$

In the particular case of the potential given by Eq. (40), we find that in  $D$  dimensions

$$g(c) = \frac{1}{(2\pi)^{D/2} \Gamma\left(\frac{D}{2}\right)} \int_0^\infty du \frac{c \exp(-u) u^{D/2-1}}{1 + c \exp(-u)}. \quad (52)$$

In the case  $D=2$ , we obtain

$$\kappa_e^{(\text{one-loop})} = \kappa + \frac{\kappa}{4\pi\rho} \left[ \ln(1 + \rho\beta) - 2 \ln\left(1 + \frac{\rho\beta}{2}\right) \right]. \quad (53)$$

However, this expression becomes negative when  $\beta$  is large, although this is outside the range where the approximation involved here is valid. We also see that  $\kappa_e$  is a nonmonotonic function of  $\rho$ , having a minimum value at some value  $\rho_c$  but increasing up to  $\kappa$  again on taking  $\rho$  very large, this is a consequence of the use of a soft potential, at high densities the particles all overlap but the energy change in moving to overlap with one particle rather than another is zero. The effective potential seen by the particles is almost flat and hence there is only a small effect on the particle diffusion.

## B. One-loop renormalization group

We have seen in the preceding section that the one-loop calculation of  $\kappa_e$  predicts that the diffusion constant can vanish at finite temperature. The same calculation predicts a van-

ishing diffusion constant for the problem of diffusion in a Gaussian random potential with short range correlations. This transition can be shown to be absent in finite dimensions via exact results in one and two dimensions, numerical simulations, and general arguments based on the fact that the system has a finite correlation length. In order to go beyond the simple one-loop contribution, one can look at how the effect of the interactions on the diffusion constant propagates from short to large length scales. This can be achieved by the renormalization-group method. This approach has been proven to be very accurate in the calculation of the effective diffusivity in random media and removes the fictitious vanishing of  $\kappa_e$  predicted by simple perturbation theory. Indeed, in dimension three the one-loop renormalization-group analysis provides a very good quantitative approximation of the effective diffusivity of a particle in a Gaussian random potential [30–34], and the exact result in dimensions one and two [35]. We therefore apply the same technique to the problem of interacting particles studied here. The potential  $\phi$  is decomposed into long and short scale components,

$$\begin{aligned} \phi_{<}(\mathbf{x}) &= \int_{|q|<\Lambda} \frac{d\mathbf{q}}{(2\pi)^{ND}} \tilde{\phi}(\mathbf{q}) \exp(i\mathbf{q} \cdot \mathbf{x}), \\ \phi_{>}(\mathbf{x}) &= \int_{|q|>\Lambda} \frac{d\mathbf{q}}{(2\pi)^{ND}} \tilde{\phi}(\mathbf{q}) \exp(i\mathbf{q} \cdot \mathbf{x}), \end{aligned} \quad (54)$$

where  $\Lambda$  is a running cutoff. One then integrates out the high momentum component  $\phi_{>}$  perturbatively to find an effective theory on length scales greater than  $1/\Lambda$ . One then makes a self-similarity ansatz which means only keeping interactions that were in the original problem and hence the only parameters which change are  $\kappa$  and  $\lambda$  (as well as the potential which just has the higher Fourier modes removed). One therefore has a running diffusion constant  $\kappa(\Lambda)$  and a running coupling to the gradient field  $\lambda(\Lambda)$ . The effective diffusion constant is then given by  $\kappa_e = \kappa(0)$ . The flows of these couplings can be computed from the one-loop diagrams. In addition it can be shown by general arguments [35] that

$$\frac{\kappa(\Lambda)}{\lambda(\Lambda)} = \frac{\kappa}{\lambda} = T, \quad (55)$$

that is to say that the Einstein relation or fluctuation dissipation relation is satisfied by the renormalized theory at each step of the renormalization. This renormalization is only valid for the low-momentum component of the remaining drift  $\nabla \phi_{<}$  and a possible improvement to the calculation here would be to functionally renormalize the field  $\phi_{<}$ , which amounts to introducing new interactions generated by the renormalization procedure (this approach has been applied to diffusion in an incompressible quenched Gaussian velocity field [36]). Using the one-loop diagrams calculated in the previous section we find the flow equation for  $\kappa(\Lambda)$  is

$$\begin{aligned} \frac{d\kappa^{(\text{one-loop})}(\Lambda)}{d\Lambda} &= -\frac{\rho\lambda(\Lambda)^2}{D\kappa(\Lambda)(2\pi)^D} S_{D-1} \Lambda^{D-1} \tilde{V}(\Lambda)^2 \\ &\times \left( \frac{1}{1 + \frac{\rho\lambda(\Lambda)}{\kappa(\Lambda)} \tilde{V}(\Lambda)} - \frac{1}{2} \frac{1}{1 + \frac{\rho\lambda(\Lambda)}{2\kappa(\Lambda)} \tilde{V}(\Lambda)} \right), \end{aligned} \quad (56)$$

where  $S_{D-1}$  is the area of the unit sphere of  $\mathbb{R}^D$ . Inserting Eq. (55) into Eq. (56) one gets

$$\begin{aligned} \frac{d\kappa^{(\text{one-loop})}(\Lambda)}{d\Lambda} &= -\frac{\rho\lambda(\Lambda)}{DT(2\pi)^D} S_{D-1} \Lambda^{D-1} \tilde{V}(\Lambda)^2 \\ &\times \left( \frac{1}{1 + \frac{\rho}{T} \tilde{V}(\Lambda)} - \frac{1}{2} \frac{1}{1 + \frac{\rho}{2T} \tilde{V}(\Lambda)} \right). \end{aligned} \quad (57)$$

Integrating out  $\Lambda$  down from  $\infty$  to 0 and using the initial conditions  $[\kappa(\infty), \lambda(\infty)] = (\kappa, \lambda)$ , we find the final expression for the effective diffusion constant is simply

$$\kappa_e^{(\text{one-loop RG})} = \kappa \exp\left(\frac{\kappa_e^{(\text{one-loop})}}{\kappa} - 1\right). \quad (58)$$

Now looking at  $\kappa_e^{(\text{one-loop})}$  given in Eq. (47), the value of the self-diffusion constant given by the self-similarity ansatz leads to several comments.

The temperature-density dependence of  $\kappa_e/\kappa$  is of the form  $h(\rho/T)/T$ . Hence the phase diagram in the  $(T, \rho)$  plane obtained from it consists of regions separated by straight lines crossing at the point  $(0, 0)$ . However, the Langevin approach studied here is in most physical situations a coarse grained approach, in which case the potential  $V$  has to be replaced by an effective potential  $V_{\text{eff}}(\mathbf{x}) = V_{\text{eff}}(\mathbf{x}, c, \rho)$  which depends on the temperature and possibly the density. In this case, the phase diagram will be more complicated.

If the Fourier transform  $\tilde{V}(q)$  of the potential has an absolute minimum of *negative value* at some nonzero value  $q^*$ , then the diffusion constant goes to zero when the temperature reaches  $T^* = -\rho[\tilde{V}(q^*)^{-1}]$  from above. Keeping the density fixed lowering  $T$  amounts to increasing  $c$ . The integral

$$I = \int d\mathbf{q} \frac{c\tilde{V}(\mathbf{q})}{1 + c\tilde{V}(\mathbf{q})} \quad (59)$$

diverges at  $c = c^* = \rho/T^*$ , and near  $c^*$  the denominator of the integrand  $I$  behaves as

$$\begin{aligned} &\{1 + (c^* - \delta c)[V(q^*) + V_{,qq}(q^*) \delta q^2/2]\} \\ &= [-\delta c V(q^*) + V_{,qq}(q^*) \delta q^2/2], \end{aligned} \quad (60)$$

where we have assumed that  $V$  is twice differentiable about  $q^*$ , i.e., the minimum is not a cusp. In this case the relaxation time diverges at  $T^*$  as

$$\tau \sim \exp\left(\frac{A}{\sqrt{T-T^*}}\right). \quad (61)$$

However, one could conceive that  $V$  is an effective potential coming from a coarse grained approach to a microscopic model and that it may thus have a dependence on  $\rho$  or  $T$ . Alternatively one might argue that diagrams of lower order in  $\rho$  dress the effective interaction leading to an additional  $\rho$  or  $T$  dependence in  $V$ . The assumption of an effective  $T$  dependence on  $V$  will modify the way in which the diffusion constant vanishes. We note here that the idea of an effective  $T$  dependence of the effective interaction arises in the random phase approximation [29] where the bare two particle interaction  $V(\mathbf{r})$  is replaced by  $-Tc(\mathbf{r})$ , where  $c(\mathbf{r})$  is the direct correlation function. In this scenario, if we keep  $\rho$  fixed, the denominator of the integrand  $I$  now behaves as

$$\begin{aligned} & \{1 + (c^* - \delta c)[V(q^*, c^*) - V_{,c}(q^*, c^*)\delta c + V_{,cc}(q^*, c^*)\delta c^2/2 \\ & \quad + V_{,cq}(q^*, c^*)\delta q^2/2 + V_{,qc}(q^*, c^*)\delta c \delta q]\} \\ & \approx [\delta c/c^* - c^*V_{,c}(q^*, c^*)\delta c - V_{,qc}(q^*, c^*)\delta c \delta q]. \end{aligned} \quad (62)$$

By definition we have that  $V_{,c}(q^*, c^*) < 0$  as the minimum of  $V(q, c)$  arrives at  $-1/c$  from above. Hence in this case the relaxation time diverges as

$$\tau \sim \exp\left(\frac{A}{T-T^*}\right), \quad (63)$$

which is the Vogel-Fulcher-Tammann law. From the above analysis we see that if the dependence of  $V(q, c)$  on  $c$  is weak near  $(q^*, c^*)$  then one would expect to see a crossover between the behavior of  $\tau$  between Eq. (61) for  $|T-T^*| < 1$ , to the behavior Eq. (63) when  $|T-T^*| \ll 1$ . The two scenarios above correspond to the behavior of the so-called fragile glasses. In the scenario where the denominator of the integrand  $I$  does not diverge then the diffusion constant only vanishes at  $T=0$  and it is possible that such cases correspond to strong glasses; however, generally the precise behavior of  $\kappa_e$  as  $T$  goes to zero will depend on the form of  $V$ , an example of which can be seen from Eq. (53) resummed in the renormalization-group approximation. If  $q^*=0$  then the behavior is different and depends on the spatial dimension  $D$ . Finally as mentioned in the previous section on the one-loop expansion, precisely at  $T=T^*$  one expects that  $\kappa_e$  depends explicitly on  $N$ .

In the corresponding static approximation [28] it was shown that the structure function is given by

$$S(q) = \frac{1}{1 + c\tilde{V}(q)}, \quad (64)$$

although the authors of [28] express  $S$  in terms of the Mayer function of the potential  $V$ , the result is the same at the order of accuracy of the calculation. We see that the condition above for a dynamic transition, defined by the vanishing of  $\kappa_e$ , coincides in the same approximation scheme by the appearance of a diverging correlation length and a second order phase transition. However, as pointed out in [28] this apparent second order transition may be preceded by a first order

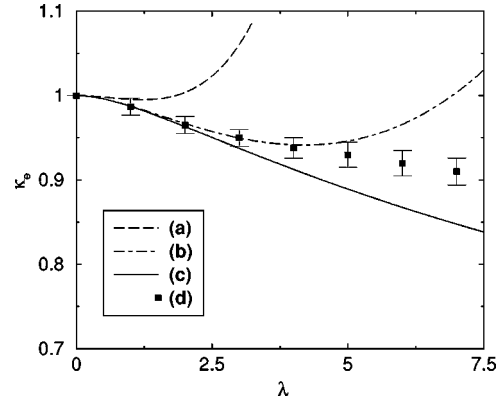


FIG. 8. Microscopic diffusion constant as a function of the interaction from different approximation schemes [(a), (b), (c)], compared to the one measured in Monte Carlo simulations:  $1/T$  expansion from Eqs. (42) and (43) (a), one-loop renormalization-group (b), one-loop renormalization-group + first two-loops diagram (c), and Monte Carlo simulations (d).

freezing transition when the free energy of the ordered crystal phase is lower than that of the free energy of the liquid phase described by the terms in the chain resummed virial expansion. The analysis above thus may apply to a supercooled liquid and the temperature  $T^*$  is the limit of the thermodynamic stability of the liquid phase. There has been some experimental evidence of a diverging correlation length at the Vogel-Fulcher-Tammann temperature  $T^*$  from the study of the dielectric susceptibility of supercooled liquids [37], though these results seem at odds with earlier numerical studies [38,39] studying this question.

#### IV. COMPARISON WITH MONTE CARLO SIMULATIONS

In order to test the accuracy of the different schemes explained above, we have carried out Monte Carlo simulations of particles interacting via the potential (40) in two dimensions. Here we have fixed the density at the value  $\rho=0.5$ , and the number of particles at  $N=10\,000$ . We have evaluated the macroscopic diffusion constant by using Eq. (3). The result is shown in Fig. 8 and compared to the evaluation from Eqs. (42) and (43), for values of the interaction in the range  $[0, 7.5]$ .

From Fig. 8 we see that the  $\beta$  expansion is valid only at very small  $\beta$ , however, the one-loop renormalization-group (RG) result is much more near the simulated values of the diffusion constant over quite a broad range. We expect that a RG analysis including more interactions, for example, including functional renormalization of the interaction  $V$ , would provide better agreement. The two-loop diagrams include the one indicated as type 1 in Fig. 5. The effect of the addition of this diagram to the one-loop RG calculation is plotted in Fig. 8 as well. The other diagrams of the two-loop expansion are at least of order  $\beta^4$ . Hence the good agreement

observed indicates that the two-loop calculation which includes additional interactions will improve the approximation to the diffusion constant. We note that the value of the density used here ( $\rho=0.5$ ) is not very small, and the reasonably good agreement obtained is a hint that the RG calculation catches the  $\rho$  dependence of the diffusion constant in the case of soft or bounded potentials.

## V. CONCLUSION

We have developed a perturbative expansion of the self-diffusion constant of Langevin interacting particles. The expansion is a weak coupling expansion which is suitable for soft or bounded interaction potentials. The perturbation expansion can be seen to be a double expansion in  $\beta$  and  $\rho$ , and we have shown how it can be dealt with diagrammatically. As an example of a partial resummation of this expansion, a one-loop renormalization group analysis has been carried out and tested on a simple form of the interaction and compared to numerical simulations. It was found that this calculation gives considerably better agreement than the straight expansion to  $O(\beta^3)$ . In addition, in some cases the one-loop RG

calculation predicts a divergence of the relaxation time (or vanishing of the self-diffusion constant) at some positive temperature. However, we have seen that when such a dynamic transition occurs it is accompanied by a diverging correlation length in the statics when one uses equivalent approximations in the statics and dynamics. The possible forms of the divergence of the relaxation time have been discussed and it has been argued that the Vogel-Fulcher-Tammann law emerges under relatively weak additional assumptions to the basic calculation carried out here. The two-loop calculation should provide a better quantitative approximation for the diffusion constant, but it would also indicate the form or robustness of the divergence of the relaxation time as higher-loop contributions are taken into account, this calculation is in progress. Various other resummation methods may be developed on the systematic perturbation expansion expounded here, as we have mentioned earlier the series may be resummed at order  $\rho$  to recover existing low density results, one may use self-consistent perturbation theory and also explore renormalization-group schemes based on calculating the effect of integrating out the effect of a small density of other particles rather than the Fourier modes of the interaction potential.

- 
- [1] C. A. Angel, *Science* **267**, 1924 (1995).
  - [2] U. Bengtzius, W. Götze, and A. Slöjander, *J. Phys. C* **17**, 5915 (1984).
  - [3] E. Leutheusser, *Phys. Rev. A* **29**, 2765 (1984).
  - [4] W. Götze, *Z. Phys. B: Condens. Matter* **56**, 139 (1984); W. Götze, *Liquids, Freezing and the Glass Transition* (Les Houches) (North-Holland, Amsterdam, 1989).
  - [5] W. Kob, *Slow Dynamics in Condensed Matter* (Les Houches) (North-Holland, Amsterdam, 2002).
  - [6] S. P. Das, G. F. Mazenko, S. Ramaswamy, and J. J. Toner, *Phys. Rev. Lett.* **54**, 118 (1985); S. P. Das and G. F. Mazenko, *Phys. Rev. A* **34**, 2265 (1986).
  - [7] W. B. Russel, D. A. Saville, and W. R. Schowalter, *Colloidal Dispersions* (Cambridge University Press, Cambridge, England, 1989).
  - [8] W. Hess and R. Klein, *Adv. Phys.* **32**, 173 (1983).
  - [9] H. Acuña-Campa and M. Medina-Noyola, *J. Chem. Phys.* **113**, 869 (2000).
  - [10] L. Yeomans-Reyna and M. Medina-Noyola, *Phys. Rev. E* **64**, 066114 (2001).
  - [11] L. Yeomans-Reyna, H. Acuña-Campa, F. de Jesús Guevara-Rodríguez, and M. Medina-Noyola, *Phys. Rev. E* **67**, 021108 (2003).
  - [12] B. J. Ackerson and L. Fleishman, *J. Chem. Phys.* **76**, 2675 (1982).
  - [13] B. U. Felderhof and R. B. Jones, *Physica A* **121**, 329 (1983); **122**, 89 (1983).
  - [14] S. Hanna, W. Hess, and R. Klein, *Physica A* **111**, 181 (1982).
  - [15] M. Medina-Noyola, *Phys. Rev. Lett.* **60**, 2705 (1988).
  - [16] G. Nägele, J. Bergenholtz, and J. K. G. Dhont, *J. Chem. Phys.* **110**, 7037 (1999).
  - [17] B. J. Ackerson, *J. Chem. Phys.* **69**, 684 (1978).
  - [18] J. A. Marqusee and J. M. Deutch, *J. Chem. Phys.* **73**, 5396 (1980).
  - [19] A. V. Indrani and S. Ramaswamy, *Phys. Rev. Lett.* **73**, 360 (1994).
  - [20] G. K. Batchelor, *J. Fluid Mech.* **74**, 1 (1976).
  - [21] G. Szamel and J. A. Leegwater, *Phys. Rev. A* **46**, 5012 (1992).
  - [22] J. A. Leegwater and G. Szamel, *Phys. Rev. A* **46**, 4999 (1992).
  - [23] H. N. W. Lekkerker and J. K. G. Dhont, *J. Chem. Phys.* **80**, 5790 (1984).
  - [24] D. Dean and A. Lefevre (unpublished).
  - [25] F. H. Stillinger, *J. Chem. Phys.* **65**, 3968 (1976); F. H. Stillinger and T. A. Weber, *ibid.* **68**, 3837 (1978); O. F. Olaj, A. Lantschbauer, and K. H. Pelinka, *Macromolecules* **13**, 299 (1980).
  - [26] M. Watzlawek, C. N. Likos, and H. Löwen, *Phys. Rev. Lett.* **82**, 5289 (1999).
  - [27] C. Marquest and T. A. Witten, *J. Phys. (France)* **50**, 1267 (1989); C. N. Likos, M. Watzlawek, and H. Löwen, *Phys. Rev. E* **58**, 3135 (1998).
  - [28] L. Acedo and A. Santos, e-print cond-mat/ 0308628.
  - [29] J. P. Hansen and I. R. McDonald, *Theory of Simple Liquids*, 2nd ed. (Academic Press, London, 1986).
  - [30] D. S. Dean, I. T. Drummond, and R. R. Horgan, *J. Phys. A* **27**, 5135 (1994).
  - [31] M. W. Deem and D. Chandler, *J. Stat. Phys.* **76**, 911 (1994).
  - [32] D. S. Dean, I. T. Drummond, and R. R. Horgan, *J. Phys. A* **28**, 1235 (1995).
  - [33] D. S. Dean, I. T. Drummond, and R. R. Horgan, *J. Phys. A* **28**, 6013 (1995).
  - [34] D. S. Dean, I. T. Drummond, and R. R. Horgan, *J. Phys. A* **29**, 7867 (1996).
  - [35] D. S. Dean, I. T. Drummond, and R. R. Horgan, *J. Phys. A* **30**,

- 385 (1997).
- [36] D. S. Dean, I. T. Drummond, and R. R. Horgan, Phys. Rev. E **63**, 061205 (2001).
- [37] N. Menon and S. R. Nagel, Phys. Rev. Lett. **74**, 1230 (1994).
- [38] R. M. Ernst, S. R. Nagel, and G. S. Grest, Phys. Rev. B **43**, 8070 (1991).
- [39] C. Dasgupta, A. V. Indrani, S. Ramaswamy, and M. K. Phani, Europhys. Lett. **15**, 307 (1991).